



## OPEN ACCESS

## EDITED BY

Quansheng Feng,  
Chengdu University of Traditional Chinese  
Medicine, China

## REVIEWED BY

Abeni Beshiru,  
Federal Institute for Risk Assessment (BfR),  
Germany  
Rosa Guillen Fretes,  
National University of Asunción, Paraguay

## \*CORRESPONDENCE

Yong Tan,  
✉ tcmpanyong@126.com  
Cheng Lu,  
✉ lv\_cheng0816@163.com  
Chunyan Jiang,  
✉ tcmjcy@126.com

<sup>†</sup>These authors share first authorship

RECEIVED 17 December 2024

ACCEPTED 12 May 2025

PUBLISHED 30 May 2025

## CITATION

Zhang L, Feng X, An H, Yang W, Xia Y, Wen B,  
Zheng H, Chen Y, Cheng Y, Jiang C, Lu C and  
Tan Y (2025) Steamed panax notoginseng  
mitigates CA-MRSA USA300-induced  
necroptosis in human neutrophils.  
*Front. Pharmacol.* 16:1546652.  
doi: 10.3389/fphar.2025.1546652

## COPYRIGHT

© 2025 Zhang, Feng, An, Yang, Xia, Wen, Zheng,  
Chen, Cheng, Jiang, Lu and Tan. This is an  
open-access article distributed under the terms  
of the [Creative Commons Attribution License  
\(CC BY\)](https://creativecommons.org/licenses/by/4.0/). The use, distribution or reproduction in  
other forums is permitted, provided the original  
author(s) and the copyright owner(s) are  
credited and that the original publication in this  
journal is cited, in accordance with accepted  
academic practice. No use, distribution or  
reproduction is permitted which does not  
comply with these terms.

# Steamed panax notoginseng mitigates CA-MRSA USA300-induced necroptosis in human neutrophils

Lulu Zhang<sup>1†</sup>, Xiaoyu Feng<sup>1†</sup>, Hongsa An<sup>1†</sup>, Weifeng Yang<sup>2</sup>,  
Yuwen Xia<sup>1</sup>, Bo Wen<sup>1</sup>, Haoran Zheng<sup>1</sup>, Yihuan Chen<sup>1</sup>,  
Yungchi Cheng<sup>3</sup>, Chunyan Jiang<sup>4\*</sup>, Cheng Lu<sup>1\*</sup> and Yong Tan<sup>1\*</sup>

<sup>1</sup>Institute of Basic Research in Clinical Medicine, China Academy of Chinese Medical Sciences, Beijing, China, <sup>2</sup>Medical Experimental Center, China Academy of Chinese Medical Sciences, Beijing, China, <sup>3</sup>Department of Pharmacology, Yale University School of Medicine, New Haven, CT, United States, <sup>4</sup>Dermatological Department, Beijing Hospital of Traditional Chinese Medicine, Capital Medical University, Beijing, China

**Background:** Community-associated methicillin-resistant *Staphylococcus aureus* (CA-MRSA) disrupts innate immunity by inducing necroptosis in polymorphonuclear neutrophils (PMNs), a process linked to excessive inflammation and tissue damage. CA-MRSA releases virulence factors that enhance its pathogenicity by disrupting the host's innate immune response, particularly impairing the phagocytic function of PMNs. Steamed Panax notoginseng (S-PN), a traditional Chinese medicine (TCM), has demonstrated immune-regulatory and anti-inflammatory properties, showing promising therapeutic effects in alleviating the severe inflammatory responses induced by pathogenic microbial infections.

**Objective:** This study aims to investigate the pharmacological effects and mechanisms of S-PN alleviating CA-MRSA-induced PMN necroptosis by suppressing MRSA virulence factors and inhibiting the RIPK1/RIPK3/MLKL signaling pathway, thereby attenuating inflammatory damage.

**Methods:** A co-culture model of MRSA USA300 strain and PMNs isolated from healthy human blood was established to observe the changes in necroptosis marker HMGB1, PMNs counts, ROS, chemokine MCP-1 and pro-inflammatory cytokines IL-1 $\beta$ , IL-8, TNF- $\alpha$ . RNA-seq was employed to analyze the effects of S-PN on the transcriptional expression of pathogenesis-related genes of MRSA. RT-PCR was utilized to validate the expression of S-PN on MRSA virulence factors and PMNs necroptosis related genes.

**Results:** S-PN significantly inhibited HMGB1, ROS, MCP-1, IL-1 $\beta$  and IL-8 in MRSA-PMN co-cultures, the PMN count in the S-PN group was higher than that in the model group. S-PN downregulated MRSA pathogenic-associated *S. aureus* infection and quorum sensing signaling pathways, and significantly reduced the virulence factors PSM and PVL. S-PN suppressed the expression of genes associated with necroptosis ripk1, ripk3, and mlkl in PMNs.

**Conclusion:** S-PN alleviates CA-MRSA infection-induced immune damage through dual mechanisms: suppression of bacterial virulence factors (PSM and PVL) and inhibition of PMNs necroptosis. These findings underscore its potential

as a complementary therapeutic strategy against CA-MRSA infections, providing a theoretical foundation for integrating TCM into adjuvant treatments for drug-resistant bacterial infections.

#### KEYWORDS

steamed *Panax notoginseng*, CA-MRSA, virulence factors, polymorphonuclear neutrophils, necroptosis

## 1 Introduction

Community-acquired methicillin-resistant *Staphylococcus aureus* (MRSA) infections pose a significant threat to global public health (Palavecino, 2020). The incidence of CA-MRSA infections has been rising annually since the 1990s, with USA300 being the predominant strain in the United States (Ahmad-Mansour et al., 2021). CA-MRSA virulence factors, such as Panton-Valentine leukocidin (PVL),  $\alpha$ -hemolysin (Hla), and phenol-soluble modulins (PSM), are critical to its pathogenicity and contribute to the impairment of innate immune responses (Tenover and Goering, 2009). The emergence of antibiotic resistance has further complicated the treatment of CA-MRSA, necessitate novel therapeutic strategies in clinical anti-infection research (Peacock and Paterson, 2015). Treatment that targets immune damage is an important part of the fight against MRSA infection.

MRSA can undermine the immune defense capacity of the host by disrupting the immune responses of immune cells (Chen et al., 2023). Clinical studies have shown that functional defects in polymorphonuclear neutrophils (PMNs) are closely associated with recurrent infections (Rungelrath and DeLeo, 2021; Warheit-Niemi et al., 2022). PMNs, as the first line of defense in innate immunity, are typically the first responders during MRSA infection, engaging in phagocytosis to eliminate the pathogen (Rungelrath and DeLeo, 2021). One of the key strategies by which MRSA disrupts the host immune response is by inducing necroptosis in PMNs. The virulence factors released by MRSA after being phagocytosed by PMNs are recognized to promote the lysis of these neutrophils (Rungelrath et al., 2021). Specifically, USA300 has been shown to induce rapid lysis of these cells, resulting in the release of damage-associated molecular patterns (DAMPs), such as HMGB1 (Irene H et al., 2015; Ludwig et al., 2023). This lysis process appears to differ from apoptosis and is characterized by features of programmed necrosis or necroptosis (Greenlee-Wacker et al., 2017; Rungelrath et al., 2021; Song et al., 2021). During this process, severe inflammatory responses and the accumulation of reactive oxygen species (ROS) are often observed, exacerbating host tissue damage (Liu et al., 2023). Developing pharmacological agents that reduce virulence factor-induced PMN necroptosis is critical to mitigate immune-mediated inflammation in CA-MRSA infections.

Traditional Chinese medicine (TCM) has been widely studied for its antibacterial effects (Yang et al., 2018; Huang et al., 2020; Zhang et al., 2021; Zhang et al., 2022). Ginseng, as a well-known TCM with clear immunoregulatory properties, has also attracted attention for its antibacterial potential (Wang et al., 2020). Asian ginseng (*Panax ginseng* C.A. Meyer), American ginseng (*Panax quinquefolius*), and *Panax notoginseng* (PN) are the three primary ginseng species globally (Wang et al., 2020). Extracts from Asian

ginseng and American ginseng have demonstrated significant inhibitory effects on the growth, adhesion, and pathogenicity of *Pseudomonas aeruginosa* (*P. aeruginosa*), *S. aureus* (*S. aureus*), and *Propionibacterium acnes* (Alipour et al., 2011; Wang et al., 2013; Zhang et al., 2014). However, most of these studies focus on the direct effects on the pathogens themselves, with little attention paid to the interaction between bacterial virulence factors and immune cell responses. Unlike the other two types of ginsengs, PN, derived from the dried roots and rhizomes of the Araliaceae family plant *Panax notoginseng* (Burk.) F.H. Chen, does not exhibit significant inhibition on bacterial growth. However, PN extracts significantly inhibit on the quorum sensing system, reducing the area of flagella motility-dependent swarming in *P. aeruginosa* (Koh and Tham, 2011). At the same time, PN, a common anti-inflammatory agent in TCM, possesses immunoregulatory and antioxidant effects (Nian-Wu et al., 2012; Liu et al., 2020; Sheng-Yan et al., 2024; Yang et al., 2024). Steamed PN (S-PN) exhibits strong pro-apoptotic effects on PMNs, promoting non-lytic apoptosis and thus clearing PMNs with minimal release of immune stimulants (such as histones and extracellular DNA) (Wang et al., 2019; Xiong et al., 2022; Yang et al., 2024). This suggests that S-PN may be an effective agent for modulating PMN immune responses and inhibiting inflammation, potentially aiding in the treatment of MRSA infections. Using an MRSA-PMN co-culture model, this study investigates the effects of S-PN on inflammatory responses and ROS accumulation in this model. RNA-seq analysis evaluates the impact of S-PN on the transcriptional expression of virulence factors in CA-MRSA USA300. Furthermore, the study explores the inhibitory effect of S-PN on the apoptosis of PMNs induced by CA-MRSA USA300. This study establishes a theoretical foundation for the clinical application of S-PN in the treatment of infectious diseases.

## 2 Materials and methods

### 2.1 Experimental reagents, bacterial strains and cells

S-PN was manufactured by Yunnan Qidan Pharmaceutical Co., Ltd., Yunnan, China. (Production Batch No: 2309003). Its preparation was performed according to the provisions of the Yunnan Province Food and Drug Administration, China (Yun YPBZ-0193-2013). The dried roots and rhizomes of PN (Araliaceae, *Panax notoginseng* (Burk.) F.H. Chen) were selected, cleaned, and steamed for 3 h. Afterward, they were dried and ground into a fine powder. The resulting powder is light yellow or brownish-yellow in color. The product quality standard stipulates that the content of total saponins of panax notoginseng (ginsenoside Rb1, ginsenoside Rg1, and ginsenoside R1) should not be less than 4.5%

(Supplementary Figure S1; Supplementary Table S1). S-PN was dissolved in Dulbecco's Modified Eagle Medium (DMEM) to prepare a 10 mg/mL S-PN solution, which was subsequently filtered through a 0.22  $\mu$ m filter membrane to remove bacteria.

The MRSA standard strain USA300 (Kansas, United States), hereafter referred to as MRSA, was purchased from American type culture collection (ATCC). The strain was stored at  $-80^{\circ}\text{C}$ . The strains were cultured on Mueller–Hinton (MH) agar broth (CM0337, Batch No. 2989738, OXOID, Britain) before use. MRSA passaging culture was performed using MH broth (CM0405, Batch No. 2963434, OXOID, Britain), which was incubated in THZ-D Desktop Constant Temperature Oscillator (Peiving Experimental Equipment Co., Ltd, Suzhou, China) at  $37^{\circ}\text{C}$  and 280 r/min with shaking until the log-phase growth was reached (16–18 h), after which the culture was diluted to  $5 \times 10^6 \sim 1 \times 10^7$  CFU/mL using fresh medium.

The Ethics Committee of the Institute of Traditional Chinese Medicine Clinical and Basic Medical Sciences, China Academy of Chinese Medical Sciences approved all peripheral blood collection procedures. PMNs were isolated from the peripheral blood of healthy volunteers using a human peripheral blood neutrophil isolation solution kit (Batch No. P9402, Solarbio). The procedure involved adding 4 mL of neutrophil separation medium to a 10 mL sterile centrifuge tube, followed by carefully layering 10 mL of EDTA-anticoagulated peripheral blood along the wall of the tube to maintain separation. The sample was then centrifuged at 500 g for 30 min, resulting in six distinct layers, with neutrophils located in the fourth layer. The plasma, mononuclear cell layer, and separation medium were carefully removed, and the neutrophil layer was collected for subsequent use.

Trypsin-EDTA was purchased from Invitrogen (Carlsbad, California, United States). Tryptone (Batch No. LP0042) and yeast extracts (Batch No. LP0021) were obtained from Oxoid, United Kingdom. NaCl (Batch No. 10019318) was from Sinopharm Chemical Reagent Co., Ltd, China.

## 2.2 Cell viability assay

CCK-8 assay was recommended for viability test. In brief, PMNs ( $1 \times 10^4$ ) were plated into a 96-well plate. Following 24 h of incubation, the medium or prepared S-PN (concentration range of 0.0312–10 mg/mL) was added to the wells and incubated for 24 h. The medium was then replaced with 100  $\mu$ L serum-free medium, and 10  $\mu$ L CCK-8 solution (Solarbio, China) was dropped into each well for 4 h of incubation. Absorbance was measured by microplate reader at 450 nm.

## 2.3 MRSA-PMN co-culture model

An *in vitro* model of MRSA-PMN infection was established based on methods reported in the literature (Chen et al., 2015; Singh et al., 2022), with modifications tailored to this study. PMNs were adjusted to a density of  $1 \times 10^4$  cells/well and uniformly seeded into plate wells. After 24 h of incubation at  $37^{\circ}\text{C}$  with 5%  $\text{CO}_2$ , the supernatant was discarded. MRSA was cultured in MH medium to  $10^8$ – $10^9$  CFU/mL, harvested by centrifugation at 3,000 rpm for

5 min, and washed three times with PBS. The bacterial pellet was resuspended in antibiotic-free DMEM. Revived MRSA was added to the wells at multiplicity of infection (MOI) ratios of 1:5, 1:10, and 1:20 (PMN:MRSA), followed by coculture at  $37^{\circ}\text{C}$  with 5%  $\text{CO}_2$  for 1, 4, and 18 h. The HMGB1 levels in the coculture supernatant were measured. MOI values and coculture durations that exhibited both elevated HMGB1 concentrations and statistically significant differences compared to other intervention conditions were selected as the optimal criteria for model establishment. Based on experimental results, an MOI of 1:10 and a 4 h coculture duration were selected as optimal parameters. For drug intervention, PMNs were pretreated with DMEM (MRSA-PMN group) or 10 mg/mL S-PN (S-PN-treated group) for 24 h prior to MRSA infection. The supernatant was then discarded, and MRSA-PMN coculture was performed as described above.

## 2.4 Enzyme-linked immunosorbent assay (ELISA)

ELISA was used to detect the secretion of HMGB1, IL-1 $\beta$ , IL-8, MCP-1, TNF- $\alpha$  in MRSA-PMN supernatants and PVL, PSM in MRSA. The sources of the kits were Human Interleukin 8 (IL-8) ELISA Kit (KQ110878), Human Tumor Necrosis Factor alpha (TNF- $\alpha$ ) ELISA Kit (KQ102647), Human Interleukin 1 $\beta$ (IL-1 $\beta$ ) ELISA Kit (KQ105768), Human Monocyte Chemotactic Protein 1 (MCP-1; CCL2) ELISA Kit (KQ110919), Human High Mobility Group Protein B1 (HMGB1) ELISA Kit (KQ105793), Bacterial phenol-soluble modulins (PSM) ELISA Kit (KQ141956) and Bacterial leucocytocide (PVL) ELISA kit (KQ141976) from Shanghai Keqiao Biotechnology Co., Ltd. Each sample was repeated three times.

## 2.5 Flow cytometry

Granulocyte counts were determined using BD FACSCalibur II™ Flow Cytometer. Granulocytes were identified and quantified by gating on the specific forward scatter (FSC) and side scatter (SSC) regions that correspond to their size and granularity. Intracellular ROS level was evaluated using the 2, 7-dichlorodihydrofluorescein diacetate (DCFH-DA) (Cat.No. D399, Thermo). Cells were stained with 1  $\mu$ L DCFH-DA for 60 min at  $37^{\circ}\text{C}$ , then washed and analyzed by flow cytometry. DCFH-DA fluorescence intensity (ex/em 488/525 nm) quantified intracellular ROS levels.

## 2.6 RNA extraction

Total RNA was extracted from three biological replicates of methicillin-resistant *S. aureus* (MRSA) in both control and S-PN-treated groups using TRIzol reagent (Invitrogen, CA, United States), followed by DNase I digestion (Takara, Japan) to eliminate genomic DNA. RNA integrity was rigorously verified through 1% agarose gel electrophoresis and Agilent 2,100 Bioanalyzer analysis (RIN  $\geq 8.0$ ; 28S/18S ratio  $>1.8$ ), with quantification performed on a NanoDrop spectrophotometer (OD260/280 = 1.8–2.2).

## 2.7 RNA-seq

Sequencing libraries were constructed with NEBNext® Ultra™ RNA Kit (NEB) following poly-A selection and cDNA synthesis protocols, and sequenced on Illumina NovaSeq 6,000 (150 bp paired-end). Raw reads were preprocessed through adapter trimming (Trimmomatic; LEADING/TRAILING:20) and quality filtering (Phred score  $\geq$  Q20), then aligned to the *S. aureus* USA300\_TCH1516 reference genome (NCBI Assembly GCA\_000017885.1) using STAR (v2.7.9a) with  $\leq 1$  mismatch. SNP calling was performed using GATK3 HaplotypeCaller after duplicate removal (Picard v1.41) and base quality recalibration.

## 2.8 Bioinformatics analysis

Gene expression quantification using HTSeq (v0.5.4) generated FPKM-normalized counts through union counting mode with reverse strand specificity. Differentially expressed genes (DEGs) were identified using DESeq (v1.10.1) with a negative binomial model, requiring  $|\log_2(\text{fold change})| \geq 1$  and Benjamini–Hochberg adjusted  $P < 0.05$ . Functional enrichment of differentially expressed genes was assessed by Goseq (v1.34.0) with Wallenius distribution-based length bias correction and KOBAS 3.0 using the *S. aureus* USA300 KEGG pathway database (sau00001), applying hypergeometric testing with Benjamini–Yekutieli FDR correction (FDR  $< 0.1$ ).

## 2.9 Quantitative real-time PCR (qRT–PCR)

Total RNA was extracted using TRIzol reagent, and its quality was assessed with a NanoDrop spectrophotometer. cDNA was synthesized from 1  $\mu\text{g}$  of RNA using HiScript III 1st Strand cDNA Synthesis Kit (+gDNA wiper) (R312-01, Nanjing Nuoweizan Biotechnology Co., Ltd). qRT–PCR was performed in a 20  $\mu\text{L}$  reaction containing SYBR Green PCR Master Mix, primers (200 nM each), and cDNA template. The genes tested with MRSA as samples were *pvl*, *psma1*, *psma2*, *psma3*, *psma4* and the reference gene was 16s rRNA. The genes tested with PMNs as samples were *ripk1*, *ripk3*, *mlkl*, *caspase-8*, *smac*, *spata2* and the reference gene was *gapdh*. The primer sequences used are shown in the [Supplementary Table S2](#). The cycling conditions included an initial denaturation at 95°C for 10 min, followed by 40 cycles of 95°C for 15 s, annealing at the optimal temperature for 30 s, and extension at 72°C for 30 s. Gene expression was quantified using the  $\Delta\Delta\text{Ct}$  method, normalizing to reference gene.

## 2.10 Statistical analysis

Data are expressed as mean  $\pm$  SD. Normality was assessed via Shapiro–Wilk test. For comparisons between two groups, unpaired Student's *t*-test (parametric) or Mann–Whitney *U* test (non-parametric) was applied. One-way ANOVA with Tukey's post-hoc test (parametric) or Kruskal–Wallis with Dunn's test (non-parametric) was used for multi-group comparisons. Adjusted *P* values  $< 0.05$  were considered significant. Analyses were performed using GraphPad Prism v10.0.

## 3 Results

### 3.1 Effects of S-PN on PMNs in MRSA-PMN Co-culture

HMGB1 levels increased significantly in MRSA-exposed PMNs versus uninfected controls. At an MOI of 1:10 and an infection duration of 4 h, the levels of HMGB1 were elevated to a greater extent compared to MOIs of 1:5 or 1:20, or infection durations of 1 h or 18 h. Based on these data, an MOI of 1:10 and an infection duration of 4 h were selected as the conditions for establishing the MRSA-PMN model in subsequent experiments ([Supplementary Figure S2A](#)).

The MIC and MBC assays revealed that S-PN does not exhibit inhibitory effects on the growth of MRSA ([Supplementary Figure S2B,C](#)). In the evaluation of drug effects on the cell viability of PMNs, it was observed that S-PN exhibits cytotoxicity at concentrations exceeding 1 mg/mL, with a cell growth inhibition rate greater than 10% ([Figure 1A](#)). Treatment with 1 and 0.5 mg/mL S-PN resulted in a significant reduction in HMGB1 level in the MRSA-PMN system post-infection, compared to the untreated Model (MRSA-PMN) group ( $P < 0.05$ ). These results suggest that S-PN protected PMNs from MRSA-induced damage ([Figure 1B](#)). In subsequent experiments of this study, 0.5 mg/mL S-PN, which exhibits no significant cytotoxicity to PMNs and effectively suppresses the MRSA-induced elevation of HMGB1 under PMN damage, will be selected as the optimal experimental drug concentration.

### 3.2 Inhibition of MRSA-Induced PMN inflammatory response by S-PN

S-PN was investigated for its inhibitory effects on MRSA-induced PMN inflammatory responses by assessing PMN inflammatory marker levels. Compared to the Control group, the levels of IL-1 $\beta$ , IL-8, and MCP-1 were significantly elevated in the Model group. In the S-PN group, IL-1 $\beta$  and MCP-1 showed a decreasing trend ([Figure 1C](#)). There were no significant differences in TNF- $\alpha$  levels between the Model and S-PN groups compared to the Control group. These results indicate that S-PN has a certain inhibitory effect on PMN inflammatory damage, reducing the release of MRSA-induced PMN pro-inflammatory factors.

### 3.3 Alleviation PMN apoptosis and ROS accumulation by S-PN

The cell numbers of PMNs and intracellular ROS levels were assessed to further determine the effects of MRSA on PMN-induced cell death and oxidative damage. The results showed that the number of granulocytes in the Model group was significantly reduced compared to the Control group, but this reduction was reversed following S-PN intervention ([Figures 1D,E](#); [Supplementary Figure S3](#)). Analysis using DCFH-DA revealed a significant increase in ROS levels in the Model group compared to the Control group, while the S-PN group exhibited a notable decrease in ROS levels ([Figures 1F,G](#); [Supplementary Figure S3](#)). These findings suggest that S-PN effectively reverses MRSA-induced oxidative damage in PMNs.



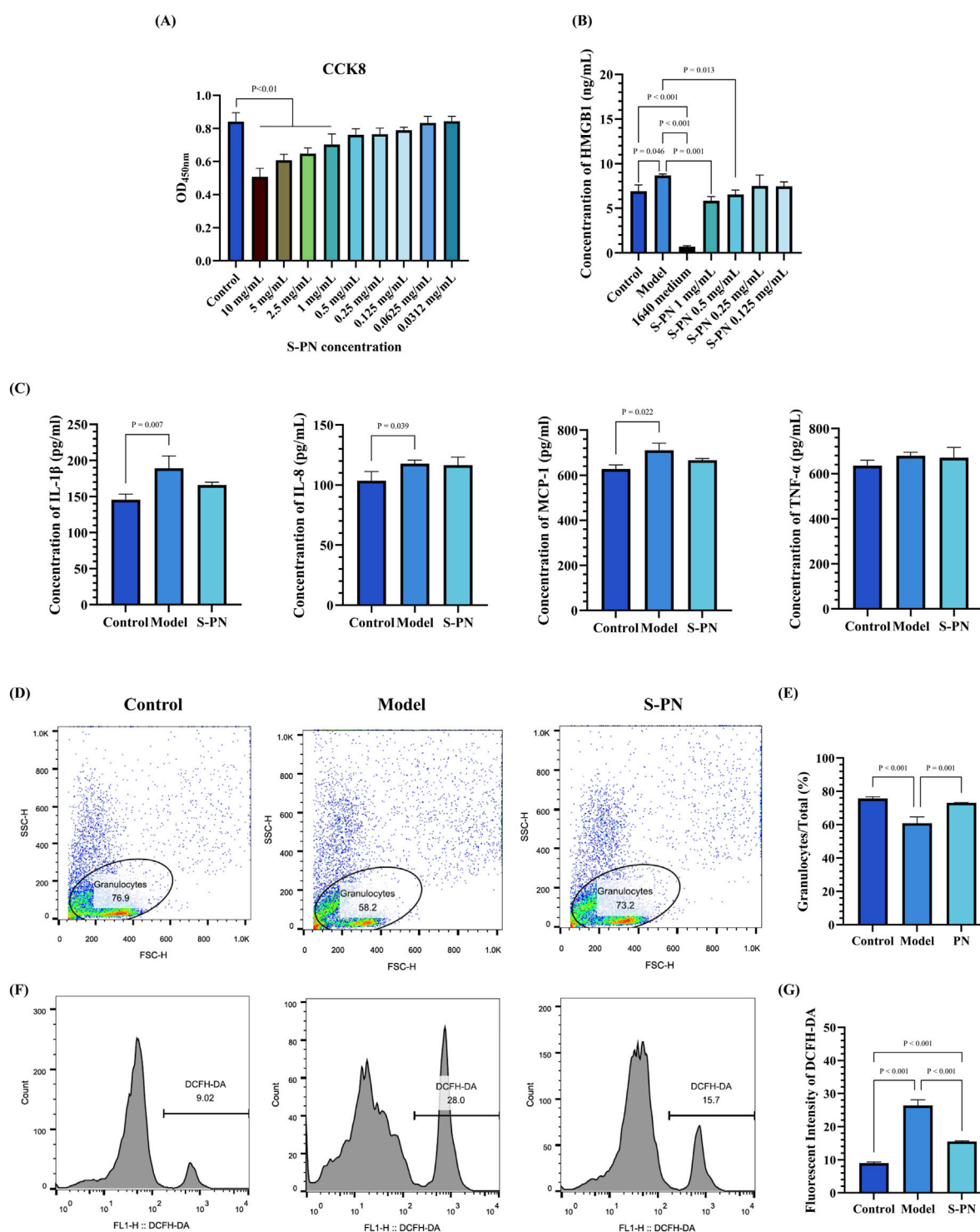


FIGURE 1

Effect of S-PN on PMNs. (A) Cytotoxicity of S-PN on PMNs. (B) Impact of S-PN on HMGB1 level released by PMNs in the MRSA-PMN model. (C) Expression levels of inflammatory cytokines in the MRSA-PMN model. (D,E) Flow cytometry analysis of the proportion of total PMNs in each group ( $n = 3$ ). (F,G). Flow cytometry analysis of ROS levels in each group ( $n = 3$ ).

### 3.4 Inhibition of MRSA virulence factor-related pathways by S-PN

To determine whether the anti-inflammatory effect of S-PN on MRSA-induced inflammation in PMNs is associated with

transcriptional suppression of MRSA genes, RNA-seq was performed to analyze the transcriptome of MRSA USA300 strain before and after S-PN intervention. A total of 2033 genes were detected. Among these, 1826 genes were common to both the Control and S-PN groups, 180 genes were exclusively found in

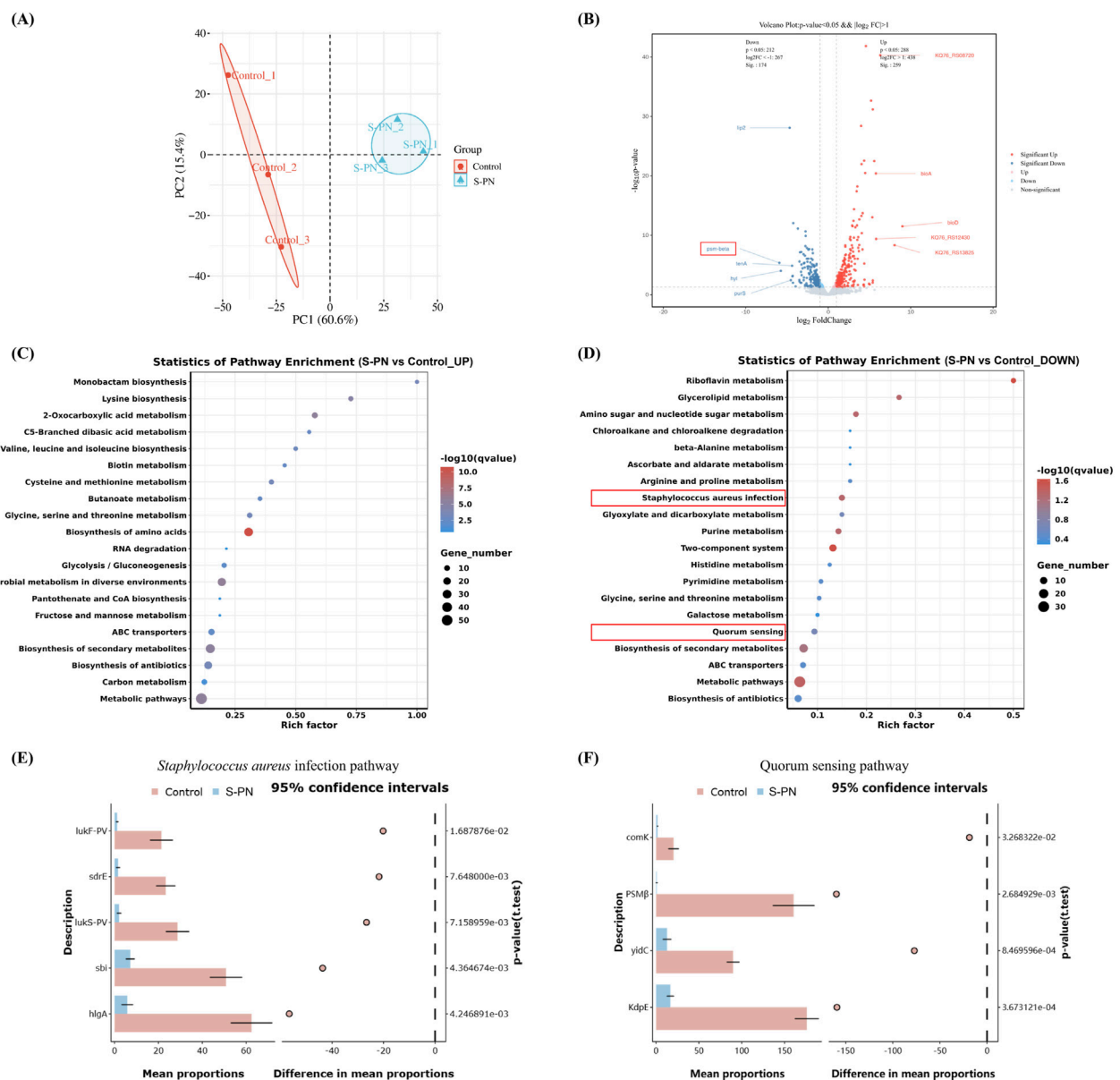


**FIGURE 2** Effect of S-PN on MRSA Gene Transcription. **(A)** Principal Component Analysis (PCA) showing significant differences in gene transcription between MRSA with S-PN intervention (S-PN group) and MRSA without intervention (Control group). **(B)** The volcano plot. S-PN vs. Control, with red indicating significantly upregulated genes and blue indicating significantly downregulated genes ( $P < 0.05$ ,  $|\log_2 \text{FC}| > 1$ ). The top 10 genes with the most significant changes are labeled on the plot. **(C,D)** KEGG pathway analysis showing significantly upregulated and downregulated pathways using STAMP. **(E,F)** The difference expression levels of hub gene in each group in *Staphylococcus aureus* infection and Quorum sensing pathway using STAMP.

the Control group, and 27 genes were unique to the S-PN group (Supplementary Figures S4A,B). Significant transcriptional differences between the two groups were observed, with 276 DEGs identified (Figure 2A; Supplementary Table S3). Following S-PN intervention, 161 DEGs such as *uspA*, *bioA*, *bioD*, and *ribU* were significantly upregulated, while 115 DEGs including *psm-beta* (*psmβ*), *lip2*, *tenA*, *hly*, and *purS* were significantly downregulated (Figure 2B; Supplementary Figure S4B).

Gene Ontology (GO) enrichment analysis revealed that the upregulated DEGs were primarily associated with biological processes (e.g., oxidation-reduction processes, carboxylic acid

metabolic processes, and oxygen-containing compound metabolic processes), cellular components (e.g., ribosomes), and molecular functions (e.g., oxidoreductase activity and ribosome structural constituent). In contrast, the downregulated DEGs were predominantly linked to biological processes (e.g., lipid biosynthesis processes, vitamin metabolic processes, and water-soluble vitamin metabolic processes) and molecular functions (e.g., 3-beta-hydroxy-delta5-steroid dehydrogenase activity and steroid dehydrogenase activity with CH-OH group donors and NAD or NADP as acceptors) (Supplementary Figures S4C,D; Supplementary Table S4).

KEGG pathway enrichment analysis indicated that the upregulated DEGs were significantly enriched in amino acid metabolism pathways (e.g., lysine biosynthesis, cysteine and methionine metabolism, and valine, leucine, and isoleucine biosynthesis), carbon and sugar metabolism pathways (e.g., glycolysis/gluconeogenesis and butyrate metabolism), and other specific metabolism pathways (e.g., 2-oxoacid metabolism and C5-branched dibasic acid metabolism). Conversely, the downregulated DEGs were primarily enriched in vitamin metabolism pathways (e.g., riboflavin metabolism), carbon and sugar metabolism pathways (e.g., glycerolipid metabolism and amino sugar and nucleotide sugar metabolism), as well as pathogen infection and signaling pathways (e.g., *S. aureus* infection and quorum sensing) (Figures 2C,D; Supplementary Table S5).

The genes enriched in these two pathways of pathogen infection and signaling are *lukF-PV*, *lukS-PV*, *sdrE*, *sbi*, *hlgA*, and *clfB* (*S. aureus* infection), as well as *psm $\beta$* , *ribD*, *sspA*, *comK*, *KdpE*, and *yidC* (Quorum sensing) (Supplementary Figure S5). Functionally, these genes are associated with pathogenicity-related processes such as cytolysis [*psm $\beta$*  (Ebner et al., 2017), *LukF-PV* (Okolie et al., 2013), *LukS-PV* (Okolie et al., 2013), *hlgA* (Venkatasubramaniam et al., 2018)], immune interference [*sbi* (Gonzalez et al., 2019), *sspA* (Oscarsson et al., 2006)], and bacterial adhesion and colonization [*sdrE* (Paiva et al., 2023), *clfB* (Xue et al., 2012)], as well as non-pathogenicity-related processes including bacterial genetic metabolism [*comK* (Turgay et al., 1997), *yidC* (Li et al., 2014), *ribD* (Miao et al., 2024)] and osmotic regulation [*KdpE* (Freeman et al., 2013)].

We observed that following S-PN intervention, the expression levels of cytolytic virulence factor genes, including *psm $\beta$*  (log2FC = -5.92), *LukF-PV* (log2FC = -2.28), *LukS-PV* (log2FC = -1.85), and *hlgA* (log2FC = -1.83), were significantly downregulated (Supplementary Figure S3E,F; Supplementary Figures S5A,C). *LukF-PV* and *LukS-PV* encode the CA-MRSA hallmark virulence factor PVL, while *psm $\beta$*  encodes PSM. PSM has been shown to enhance the lytic activity of PVL against PMNs (Hongo et al., 2009), whereas *hlgA* is primarily associated with erythrocyte lysis. Based on these findings, this study focuses on investigating the impact of S-PN on PVL- and PSM-mediated PMN apoptosis during CA-MRSA infection.

### 3.5 Inhibition of MRSA virulence factors PSM and PVL expression by S-PN

The impact of S-PN on the expression of MRSA virulence factors PSM and PVL was assessed using PCR and ELISA. The mRNA transcription levels of *pvl*, *psm  $\alpha$ 1*,  *$\alpha$ 2*,  *$\alpha$ 3*, and  *$\alpha$ 4* in the S-PN group were significantly reduced compared to the Control group (Figure 3A). Similarly, the concentration levels of PVL and PSM in cells were markedly decreased in the S-PN group compared to the Control group (Figure 3B). These results indicate that S-PN exerts a suppressive effect on both the transcription and expression of MRSA virulence factors PSM and PVL. Therefore, S-PN may reduce the pathogenicity of MRSA by modulating its virulence factors.

### 3.6 Inhibitory effects of S-PN on the RIPK1/RIPK3/MLKL pathway induced by MRSA in PMNs

To further explore the specific mechanisms by which MRSA virulence factors induce damage in PMNs, we examined the expression levels of genes associated with RIPK1/RIPK3/MLKL necroptotic signaling pathway in PSM-induced PMNs. Necrostatin-1s (Nec-1s), an RIPK1 inhibitor, was used as a control (Supplementary Figure S2D). Both the S-PN and Nec-1s groups exhibited similar inhibitory effects on HMGB1 compared to the Control group, indicating that suppression of the necroptotic pathway can mitigate PMN damage (Figure 4A). In terms of gene expression related to the necroptotic pathway, the mRNA levels of *ripk1*, *ripk3*, and *mlkl* were significantly elevated in the model group, suggesting that MRSA induces necroptosis in PMNs. Following S-PN intervention, the mRNA levels of *ripk1*, *ripk3*, and *mlkl* were significantly reduced, with *ripk1* and *ripk3* levels comparable to those in Nec-1s group (Figure 4B). These results suggest that S-PN may regulate PMN necroptosis by inhibiting the transcription of *ripk1*, *ripk3*, and *mlkl* mRNA.

This finding was further corroborated by analyzing the mRNA expression of relevant regulators of the RIPK1/RIPK3/MLKL pathway, including caspase-8, smac, and spata2 (Figure 4B). Compared to the Control group, the expression of smac and spata2 was significantly decreased in the Model group, while caspase-8 expression also showed a decreasing trend (Figure 4B). The decreased expression of caspase-8 suggests that MRSA may promote necroptotic signaling by reducing the ability of Caspase-8 to dissociate the RIPK1/RIPK3 complex, thereby maintaining the complex and facilitating necroptosis. The decreased spata2 expression in the Model group suggests that necroptotic signaling in PMNs is not activated by MRSA through the enhancement of SPATA2-mediated RIPK1 deubiquitination. The S-PN group showed a trend of increased smac expression and similar levels of caspase-8 expression compared to the Model group, suggesting that S-PN may enhance SMAC-mediated activation of Caspase, though this activation does not appear to target caspase-8. The exact mechanism warrants further investigation.

## 4 Discussion

CA-MRSA spreads rapidly and has increasingly become predominant in community infections across various regions worldwide (Tenover and Goering, 2009). Its pathogenicity largely depends on its virulence factors. CA-MRSA virulence factors directly suppress host immune responses. As the first line of innate immunity, PMNs are particularly vulnerable to MRSA virulence factors like PSM, which can inhibit their phagocytic and bactericidal activities while inducing necroptosis (Peschel and Otto, 2013). S-PN, a commonly used anti-inflammatory agent in TCM, exhibits clear necroptosis inhibition (Hu et al., 2022). In this study, using an MRSA-PMNs co-culture model, we observed that S-PN suppressed the inflammatory response and ROS accumulation in the model. Furthermore, S-PN significantly inhibits the transcription of CA-MRSA USA300 virulence factors, including

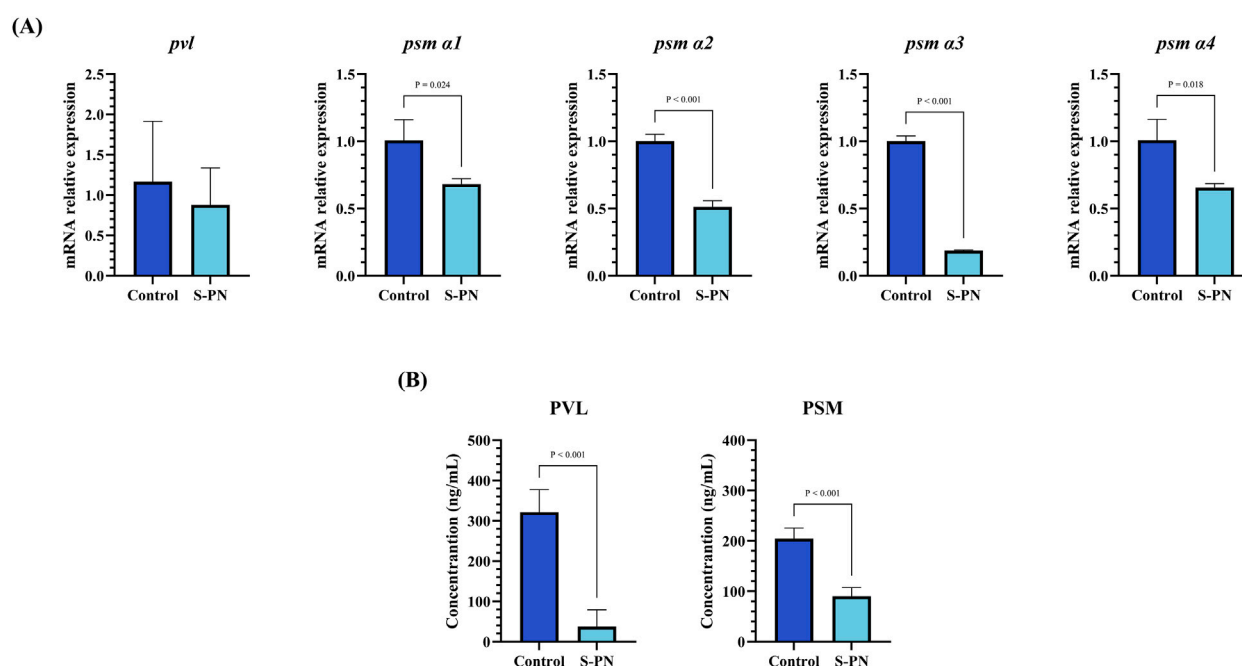


**FIGURE 3**  
Effect of S-PN on MRSA virulence factors PSM and PVL expression. **(A)** The mRNA expression levels of MRSA virulence factors *psm α1*, *psm α2*, *psm α3*, *psm α4* and *pvl*. **(B)** The protein expression levels of MRSA virulence factors PSM and PVL.

PSM and PVL, and reduces the expression of pathogen infection-related pathways, including quorum sensing. This leads to the suppression of necroptotic signaling pathways induced by PSM in PMNs.

PMNs are the most abundant white blood cells in the circulatory system, and their phagocytic activity is crucial for the clearance of invading MRSA. The surface Toll-like receptors (TLRs) on PMNs recognize various surface-associated or freely secreted molecules produced by MRSA, thereby activating phagocytosis of MRSA (Hayashi et al., 2003). Intracellular ROS disrupt bacterial redox homeostasis, inducing lethal oxidative stress (Valko et al., 2007). However, excessive ROS can also be released into the extracellular environment, leading to localized tissue damage at the infection site (Figure 5). Research has demonstrated that ROS can induce permanent changes in the expression of inflammatory genes through redox signaling (Wright et al., 2010). Additionally, ROS can activate the NLRP3 inflammasome, leading to the cleavage of inflammatory cytokine precursors pro-IL-1 $\beta$  and pro-IL-18 into their active forms (IL-1 $\beta$ , IL-18) (Zhou et al., 2010). To prevent severe inflammatory responses and damage to host cells and tissues caused by excessive ROS accumulation, regulating the balance of ROS within PMNs is crucial for effective anti-infection therapy (Figure 5). S-PN demonstrates potent free radical scavenging (Xiong et al., 2019). Our findings confirm its antioxidative efficacy in combating CA-MRSA infection, with significantly reduced ROS accumulation levels observed in MRSA-PMN following S-PN intervention.

Current studies have confirmed that reducing excessive ROS production in glioblastoma cells can decrease pro-inflammatory factors IL-8 and MCP-1, thereby preventing the establishment of a harmful pro-inflammatory tumor microenvironment (Tewari

et al., 2009). MCP-1 regulates immune cell recruitment (PMNs, monocytes, lymphocytes) to damaged tissues (Deshmane et al., 2009). It is primarily produced by early-infiltrating PMNs during infection. Inhibition of this chemokine can block the recruitment of immune cells to the infection site, thereby reducing excessive inflammatory responses (Yoshimura and Takahashi, 2007; Deshmane et al., 2009). In this study, MRSA caused significant damage to PMNs, with notable increases in the pro-inflammatory factors IL-1 $\beta$ , IL-8, and MCP-1. The anti-inflammatory efficacy of PN has been well-established in scientific literature. However, our results demonstrated only modest downregulation of inflammatory mediators following S-PN intervention. This attenuated effect may be attributed to alterations in bioactive components during PN processing (Xiong et al., 2019). While ginsenoside 20(S)-Rg3 has been identified as the primary bioactive component responsible for S-PN's anti-inflammatory effects, its content in S-PN is comparatively lower than unprocessed PN-derived anti-inflammatory constituents such as notoginsenoside R1, ginsenosides Rg1, Re, and Rb1 (Zhang et al., 2019). Although the intervention with S-PN did not significantly downregulate inflammatory factors. Reduced HMGB1, elevated granulocytes, and suppressed ROS collectively indicate that S-PN provides protective effects for PMNs (Figure 5).

Current research on the regulation of PMN immune function by PN primarily focuses on pathological conditions such as myocardial infarction (Li et al., 2022), ischemia-reperfusion (Rong et al., 2009), and inflammation (Xiong et al., 2022). However, the regulatory effect of S-PN on PMNs during infectious diseases, where external pathogens invade the body, has not been thoroughly explored. In the process of CA-MRSA infection, its strategy to counteract host immune defense relies on its functional agr quorum sensing



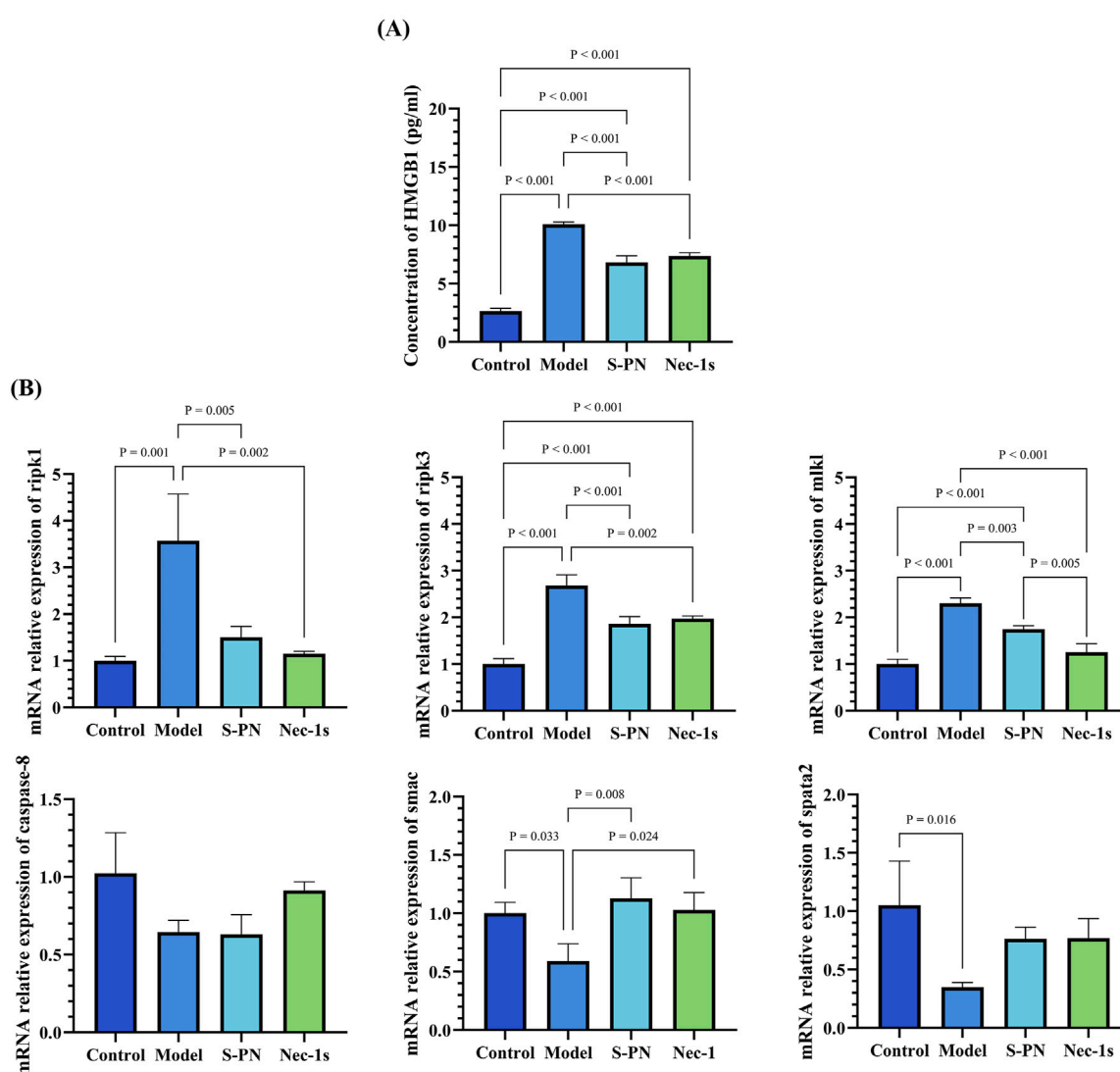
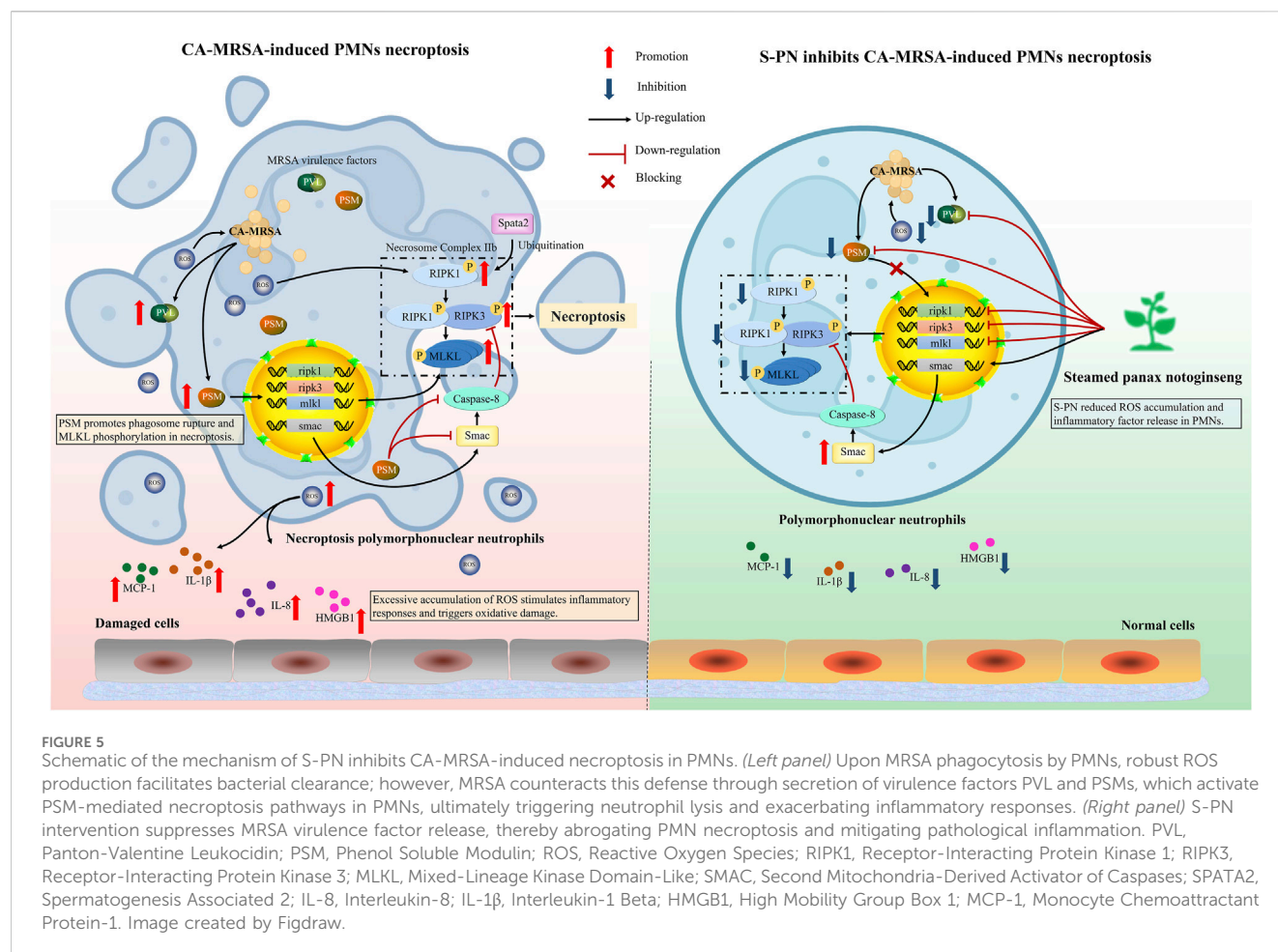


**FIGURE 4**  
Effects of S-PN on the Necroptotic Apoptosis Pathway in MRSA-PMNs. (A) Expression levels of HMGB1 in MRSA-PMNs. (B) Expression levels of genes associated with the necroptotic apoptosis pathway in PMNs.

system (Cheung et al., 2021; Cella et al., 2023). The high virulence phenotype exhibited by CA-MRSA USA300 is intricately linked to the activation of the agr system. The quorum sensing system regulates the production of virulence factors that can evade PMN-mediated killing and lead to rapid destruction of these host cells (Matsumoto et al., 2021). Our study demonstrates that S-PN significantly downregulates the quorum sensing pathway in the MRSA-PMN model, suggesting that S-PN may influence the production of virulence factors regulated by this pathway. Consequently, we further investigated the virulence factors of USA300. Traditional programmed cell death is characterized by non-lytic processes. During cell death, ‘eat me’ signals attract phagocytes to clear the dead cells without triggering an inflammatory response (Newton et al., 2024). In contrast, lytic apoptosis, including necroptosis, involves cell rupture during death, releasing cellular contents and triggering an inflammatory response (Newton et al., 2024). PVL, a two-component toxin

composed of LukF-PV and LukS-PV, has been shown to induce PMN lysis, impair host defenses, and facilitate the clearance of infected tissues (Jhelum et al., 2024). PVL-containing CA-MRSA strains typically cause tissue necrosis and leukopenia (Hofstee et al., 2024). PVL can activate the mitochondrial pathway of caspases to induce spontaneous apoptosis in PMNs (Genestier et al., 2005). However, there have been no clear reports indicating that PVL is associated with the necroptotic pathway in PMNs.

Another critical virulence factor of USA300, PSM, is an amphipathic  $\alpha$ -helical peptide with strong hemolytic activity, considered a key factor in enhancing CA-MRSA virulence (Kim et al., 2020). Different types of PSM exhibit varied effects on PMNs (Hu Z. et al., 2022). PSMa3, in particular, has notable pro-inflammatory activity, stimulating PMN chemotaxis and inducing IL-8 release (Matsumoto et al., 2021). PSMa1, PSMa2, and PSMa3 contribute to the enhanced cell-lytic activity of CA-MRSA. Compared to PSMa gene knockout mutants, wild-type



strains exhibit significantly higher lytic activity against PMNs and monocytes (Wang et al., 2007). Research reports indicate that after phagocytosing *S. aureus*, PMNs undergo dissolution, accompanied by characteristics of both apoptosis and necrosis (Chen H. et al., 2022). This is due to PSMa1, a2, and a3 inducing MLKL phosphorylation, leading to necroptotic apoptosis in PMNs (Zhou et al., 2018). The necroptosis pathway primarily involves the RIPK1 and RIPK3 proteins, which interact to activate the apoptotic program (Figure 5). RIPK complex-mediated MLKL phosphorylation drives its oligomerization and membrane translocation, where it interacts with phosphatidylinositol, triggering membrane permeabilization and cell destruction (Rickard et al., 2014; Wang et al., 2014; Chen et al., 2017). S-PN suppresses the formation of lytic programmed cell death mechanisms, such as neutrophil extracellular traps (NETosis) (Chen Z. et al., 2022). In this study, experiments were conducted to investigate whether S-PN blocks CA-MRSA-induced necroptosis, a similarly lytic form of cell death. The results demonstrated that S-PN suppresses the expression of PVL and PSM. This indicates that S-PN interferes with the induction and activation of the necroptosis pathway in PMNs by PSM through downregulating the quorum sensing pathway in USA300. Specifically, this activation is confirmed to enhance the transcription of key genes *ripk1*, *ripk3*, and *mlkl*, which is reversed by S-PN (Figure 5). The inhibitory effects on *ripk1* and *ripk3* align with those of the RIPK1 inhibitor Nec-1s,

while the suppression of *mlkl* is slightly weaker compared to Nec-1s. Nec-1s directly binds to the RIPK1 protein and inhibits its phosphorylation, thereby reducing MLKL activation (Jhun et al., 2019). Regarding the impact on necroptosis pathway-related proteins, based on existing studies, we hypothesize that PSM induces MLKL phosphorylation, promotes MLKL interaction with cell membranes, and triggers cell lysis. By suppressing PSM expression in USA300, S-PN reduces PSM-mediated MLKL phosphorylation and blocks PMN lysis. Notably, S-PN not only exhibits anti-necroptotic effects comparable to Nec-1s but also directly targets the pathogen by inhibiting the quorum sensing pathway and virulence factor expression in CA-MRSA.

Necroptosis is regulated by multiple intracellular factors. The inhibition of necroptosis is controlled by Caspase-8, which mediates the classical apoptotic pathway by cleaving RIPK1 protein to suppress its kinase activity, thereby blocking necroptosis (Weinlich et al., 2017). Smac, a caspase activator, facilitates the activation of downstream caspases and assists the Caspase-8 complex in inducing apoptosis and suppressing necrosis (Figure 5) (He et al., 2009; Green, 2022). Studies have shown that S-PN is enriched with bioactive components such as ginsenoside Rh4 and 20(S)-Rg3, which induce apoptosis in PMNs at amputation sites in zebrafish larvae (Xiong et al., 2022; Yang et al., 2024). However, our experimental results revealed that although S-PN significantly enhances smac transcription, it does not

increase caspase-8 expression, indicating that S-PN does not inhibit the necroptosis pathway via Caspase-8-mediated RIPK1 cleavage. Further studies demonstrate that active components in S-PN, including ginsenoside F4 and ginsenoside Rg6, exert significant regulatory effects on the mitochondria-dependent apoptotic protein Bax and the anti-apoptotic protein Bcl-2 (Chen and Jia, 2013; Chen et al., 2013). We hypothesize that S-PN may activate the classical apoptotic pathway by upregulating Bax and suppressing Bcl-2, thereby inhibiting necroptosis. Additionally, Spata2, a deubiquitinating enzyme for M1 ubiquitin chains of RIPK1, promotes necroptosis by enhancing RIPK1 kinase activity (Wei et al., 2017). MRSA suppresses *spata2* transcription, suggesting that its promotion of PMN necroptosis does not rely on modulating RIPK1 ubiquitination. Nevertheless, whether MRSA or its virulence factor PSM directly regulates RIPK1 requires further investigation.

## 5 Conclusion

The induction of PMN necroptosis by CA-MRSA virulence factors is one of the key challenges in treating MRSA infections. During CA-MRSA infection, severe inflammatory responses caused by ROS accumulation in PMNs also contribute to tissue damage. S-PN reduces ROS levels in PMNs, inhibits the release of inflammatory cytokines IL-1 $\beta$  and IL-8, and suppresses the production of the chemokine MCP-1. By downregulating the quorum sensing system, S-PN inhibits the production of CA-MRSA virulence factors PVL and PSM, thereby blocking PSM-induced necroptosis in PMNs. This results in reduced expression of *ripk1*, *ripk3*, and *mlkl*, ultimately diminishing CA-MRSA's pro-necroptotic effects on PMNs. This study demonstrates that S-PN protects host immune defenses by suppressing CA-MRSA virulence factor release, thereby preserving PMN-mediated immune functions and mitigating tissue injury caused by excessive inflammation. Future research will focus on validating S-PN's therapeutic efficacy against CA-MRSA infections in *in vivo* models. Our findings provide a theoretical foundation for the clinical application of traditional Chinese medicine in antibacterial therapy.

## Data availability statement

The data presented in the study are deposited in the Gene Expression Omnibus (GEO) database, accession number GSE284429.

## Ethics statement

The studies involving humans were approved by the Ethics Committee of the Institute of Traditional Chinese Medicine Clinical and Basic Medical Sciences, China Academy of Chinese Medical Sciences. The studies were conducted in accordance with the local legislation and institutional requirements. The participants provided their written informed consent to participate in this study.

## Author contributions

LZ: Conceptualization, Data curation, Methodology, Writing – original draft. XF: Conceptualization, Methodology, Writing – review and editing. HA: Formal Analysis, Investigation, Writing – original draft. WY: Supervision, Validation, Writing – review and editing. YX: Resources, Writing – review and editing. BW: Project administration, Writing – review and editing. HZ: Software, Writing – review and editing. YiC: Visualization, Writing – review and editing. YuC: Supervision, Writing – review and editing. CJ: Conceptualization, Supervision, Writing – review and editing. CL: Conceptualization, Investigation, Supervision, Writing – review and editing. YT: Conceptualization, Funding acquisition, Supervision, Writing – original draft.

## Funding

The author(s) declare that financial support was received for the research and/or publication of this article. This work was supported by the scientific and technological innovation project of China Academy of Chinese Medical Sciences (CI2021B003, CI2021A00704-2, CI2023C065YLL); and the fundamental research funds for the central public welfare research institutes of China [Z0735].

## Conflict of interest

The authors declare that the research was conducted in the absence of any commercial or financial relationships that could be construed as a potential conflict of interest.

## Generative AI statement

The author(s) declare that no Generative AI was used in the creation of this manuscript.

## Publisher's note

All claims expressed in this article are solely those of the authors and do not necessarily represent those of their affiliated organizations, or those of the publisher, the editors and the reviewers. Any product that may be evaluated in this article, or claim that may be made by its manufacturer, is not guaranteed or endorsed by the publisher.

## Supplementary material

The Supplementary Material for this article can be found online at: <https://www.frontiersin.org/articles/10.3389/fphar.2025.1546652/full#supplementary-material>

## References

- Ahmad-Mansour, N., Loubet, P., Pouget, C., Dunyach-Remy, C., Sotto, A., Lavigne, J. P., et al. (2021). Staphylococcus aureus toxins: an update on their pathogenic properties and potential treatments. *Toxins (Basel)* 13 (10), 677. doi:10.3390/toxins13100677
- Alipour, M., Omri, A., and Suntres, Z. E. (2011). Ginseng aqueous extract attenuates the production of virulence factors, stimulates twitching and adhesion, and eradicates biofilms of *Pseudomonas aeruginosa*. *Can. J. Physiology Pharmacol.* 89 (6), 419–427. doi:10.1139/y11-057
- Cella, M. A., Coulson, T., MacEachern, S., Badr, S., Ahmadi, A., Tabatabaei, M. S., et al. (2023). Probiotic disruption of quorum sensing reduces virulence and increases cefoxitin sensitivity in methicillin-resistant Staphylococcus aureus. *Sci. Rep.* 13 (1), 4373. doi:10.1038/s41598-023-31474-2
- Chen, B., and Jia, X.-B. (2013). Apoptosis-inducing effect of ginsenoside Rg6 on human lymphocytoma JK cells. *Mol. Basel, Switz.* 18 (7), 8109–8119. doi:10.3390/molecules18078109
- Chen, B., Shen, Y.-P., Zhang, D.-F., Cheng, J., and Jia, X.-B. (2013). The apoptosis-inducing effect of ginsenoside F4 from steamed notoginseng on human lymphocytoma JK cells. *Nat. Prod. Res.* 27 (24), 2351–2354. doi:10.1080/14786419.2013.828290
- Chen, H., Wang, B., Zhao, R., Gao, D., Guan, M., Zheng, L., et al. (2015). Coculture with low-dose SWCNT attenuates bacterial invasion and inflammation in human enterocyte-like Caco-2 cells. *Small Weinheim Der Bergstrasse, Ger.* 11 (34), 4366–4378. doi:10.1002/smll.201500136
- Chen, H., Zhang, J., He, Y., Lv, Z., Liang, Z., Chen, J., et al. (2022a). Exploring the role of *Staphylococcus aureus* in inflammatory diseases. *Toxins* 14 (7), 464. doi:10.3390/toxins14070464
- Chen, S., Lv, X., Hu, B., Shao, Z., Wang, B., Ma, K., et al. (2017). RIPK1/RIPK3/MLKL-mediated necroptosis contributes to compression-induced rat nucleus pulposus cells death. *Apoptosis* 22 (5), 626–638. doi:10.1007/s10495-017-1358-2
- Chen, Y., Liu, Z., Lin, Z., Lu, M., Fu, Y., Liu, G., et al. (2023). The effect of Staphylococcus aureus on innate and adaptive immunity and potential immunotherapy for S. aureus-induced osteomyelitis. *Front. Immunol.* 14, 1219895. doi:10.3389/fimmu.2023.1219895
- Chen, Z., Wang, G., Xie, X., Liu, H., Liao, J., Shi, H., et al. (2022b). Ginsenoside Rg5 allosterically interacts with P2RY12 and ameliorates deep venous thrombosis by counteracting neutrophil NETosis and inflammatory response. *Front. Immunol.* 13, 918476. doi:10.3389/fimmu.2022.918476
- Cheung, G. Y. C., Bae, J. S., and Otto, M. (2021). Pathogenicity and virulence of Staphylococcus aureus. *Virulence* 12 (1), 547–569. doi:10.1080/21505594.2021.1878688
- Deshmane, S. L., Kremlev, S., Amini, S., and Sawaya, B. E. (2009). Monocyte chemoattractant protein-1 (MCP-1): an overview. *J. Interferon Cytokine Res.* 29 (6), 313–326. doi:10.1089/jir.2008.0027
- Ebner, P., Lugman, A., Reichert, S., Hauf, K., Popella, P., Forchhammer, K., et al. (2017). Non-classical protein excretion is boosted by psma-induced cell leakage. *Cell Rep.* 20 (6), 1278–1286. doi:10.1016/j.celrep.2017.07.045
- Freeman, Z. N., Dorus, S., and Waterfield, N. R. (2013). The KdpD/KdpE two-component system: integrating K<sup>+</sup> homeostasis and virulence. *PLoS Pathog.* 9 (3), e1003201. doi:10.1371/journal.ppat.1003201
- Genestier, A.-L., Michallet, M.-C., Prévost, G., Bellot, G., Chalabreysse, L., Peyrol, S., et al. (2005). Staphylococcus aureus Panton-Valentine leukocidin directly targets mitochondria and induces Bax-independent apoptosis of human neutrophils. *J. Clin. Investigation* 115 (11), 3117–3127. doi:10.1172/JCI22684
- Gonzalez, C. D., Ledo, C., Cela, E., Stella, I., Xu, C., Ojeda, D. S., et al. (2019). The good side of inflammation: Staphylococcus aureus proteins SpA and Sbi contribute to proper abscess formation and wound healing during skin and soft tissue infections. *Biochimica Biophysica Acta. Mol. Basis Dis.* 1865 (10), 2657–2670. doi:10.1016/j.bbdis.2019.07.004
- Green, D. R. (2022). The mitochondrial pathway of apoptosis Part II: the BCL-2 protein family. *Cold Spring Harb. Perspect. Biol.* 14 (6), a041046. doi:10.1101/cshperspect.a041046
- Greenlee-Wacker, M. C., Kremserová, S., and Nauseef, W. M. (2017). Lysis of human neutrophils by community-associated methicillin-resistant Staphylococcus aureus. *Blood* 129 (24), 3237–3244. doi:10.1182/blood-2017-02-766253
- Hayashi, F., Means, T. K., and Luster, A. D. (2003). Toll-like receptors stimulate human neutrophil function. *Blood* 102 (7), 2660–2669. doi:10.1182/blood-2003-04-1078
- He, S., Wang, L., Miao, L., Wang, T., Du, F., Zhao, L., et al. (2009). Receptor interacting protein kinase-3 determines cellular necrotic response to TNF- $\alpha$ . *Cell* 137 (6), 1100–1111. doi:10.1016/j.cell.2009.05.021
- Hofstee, M. I., Siverino, C., Saito, M., Meghwhani, H., Tapia-Dean, J., Arveladze, S., et al. (2024). Staphylococcus aureus Panton-Valentine Leukocidin worsens acute implant-associated osteomyelitis in humanized BRGSF mice. *JBM R Plus* 8 (2), ziad005. doi:10.1093/jbmrl/ziad005
- Hongo, I., Baba, T., Oishi, K., Morimoto, Y., Ito, T., and Hiramatsu, K. (2009). Phenol-soluble modulins  $\alpha$  3 enhances the human neutrophil lysis mediated by Pantone-Valentine leukocidin. *J. Infect. Dis.* 200 (5), 715–723. doi:10.1086/605332
- Hu, Y., Lei, H., Zhang, S., Ma, J., Kang, S., Wan, L., et al. (2022a). Panax notoginseng saponins protect Brain microvascular endothelial cells against oxygen-glucose deprivation/resupply-induced necroptosis via suppression of RIP1-RIP3-MLKL signaling pathway. *Neurochem. Res.* 47 (11), 3261–3271. doi:10.1007/s11064-022-03675-0
- Hu, Z., Koppurapu, P. K., Ebner, P., Mohammad, M., Lind, S., Jarneborn, A., et al. (2022b). Phenol-soluble modulins  $\alpha$  and  $\beta$  display divergent roles in mice with staphylococcal septic arthritis. *Commun. Biol.* 5 (1), 910. doi:10.1038/s42003-022-03839-2
- Huang, X., Wang, P., Li, T., Tian, X., Guo, W., Xu, B., et al. (2020). Self-assemblies based on traditional medicine berberine and cinnamic acid for adhesion-induced inhibition multidrug-resistant Staphylococcus aureus. *ACS Appl. Mater. and Interfaces* 12 (1), 227–237. doi:10.1021/acsami.9b17722
- Irene, H. H., Simon, D. P., Carin, L., Harold, G. d.B., G Jan, Z., Hester, v.d.V., et al. (2015). Cigarette smoke-induced damage-associated molecular pattern release from necrotic neutrophils triggers proinflammatory mediator release. *Am. J. Respir. Cell Mol. Biol.* 52 (5), 554–562. doi:10.1165/rcmb.2013-0505OC
- Jhelum, H., Čerina, D., Harbort, C. J., Lindner, A., Hanitsch, L. G., Leistner, R., et al. (2024). Pantone-Valentine leukocidin-induced neutrophil extracellular traps lack antimicrobial activity and are readily induced in patients with recurrent PVL + -Staphylococcus aureus infections. *J. Leukoc. Biol.* 115 (2), 222–234. doi:10.1093/jleuko/qiad137
- Jhun, J., Lee, S. H., Kim, S.-Y., Ryu, J., Kwon, J. Y., Na, H. S., et al. (2019). RIPK1 inhibition attenuates experimental autoimmune arthritis via suppression of osteoclastogenesis. *J. Transl. Med.* 17 (1), 84. doi:10.1186/s12967-019-1809-3
- Kim, D.-R., Lee, Y., Kim, H.-K., Kim, W., Kim, Y.-G., Yang, Y.-H., et al. (2020). Phenol-soluble modulins-mediated aggregation of community-associated methicillin-resistant Staphylococcus aureus in human cerebrospinal fluid. *Cells* 9 (3), 788. doi:10.3390/cells9030788
- Koh, K. H., and Tham, F.-Y. (2011). Screening of traditional Chinese medicinal plants for quorum-sensing inhibitors activity. *J. Microbiol. Immunol. Infect. = Wei Mian Yu Gan Ran Za Zhi* 44 (2), 144–148. doi:10.1016/j.jmii.2009.10.001
- Li, H., Zhu, J., Xu, Y.-W., Mou, F.-F., Shan, X.-L., Wang, Q.-L., et al. (2022). Notoginsenoside R1-loaded mesoporous silica nanoparticles targeting the site of injury through inflammatory cells improves heart repair after myocardial infarction. *Redox Biol.* 54, 102384. doi:10.1016/j.redox.2022.102384
- Li, Z., Boyd, D., Reindl, M., and Goldberg, M. B. (2014). Identification of YidC residues that define interactions with the sec apparatus. *J. Bacteriol.* 196 (2), 367–377. doi:10.1128/JB.01095-13
- Liu, H., Lu, X., Hu, Y., and Fan, X. (2020). Chemical constituents of Panax ginseng and Panax notoginseng explain why they differ in therapeutic efficacy. *Pharmacol. Res.* 161, 105263. doi:10.1016/j.phrs.2020.105263
- Liu, J., Han, X., Zhang, T., Tian, K., Li, Z., and Luo, F. (2023). Reactive oxygen species (ROS) scavenging biomaterials for anti-inflammatory diseases: from mechanism to therapy. *J. Hematol. and Oncol.* 16 (1), 116. doi:10.1186/s13045-023-01512-7
- Ludwig, N., Thörner-van Almsick, J., Mersmann, S., Bardel, B., Niemann, S., Chasan, A. I., et al. (2023). Nuclease activity and protein A release of Staphylococcus aureus clinical isolates determine the virulence in a murine model of acute lung infection. *Front. Immunol.* 14, 1259004. doi:10.3389/fimmu.2023.1259004
- Matsumoto, M., Nakagawa, S., Zhang, L., Nakamura, Y., Villaruz, A. E., Otto, M., et al. (2021). Interaction between Staphylococcus Agr virulence and neutrophils regulates pathogen expansion in the skin. *Cell Host and Microbe* 29 (6), 930–940.e4. doi:10.1016/j.chom.2021.03.007
- Miao, Y., Shuang, W., Qianwei, Q., Xin, L., Wei, P., Hai, Y., et al. (2024). Proteomic study of the inhibitory effects of tannic acid on MRSA biofilm. *Front. Pharmacol.* 15, 1413669. doi:10.3389/fphar.2024.1413669
- Newton, K., Strasser, A., Kayagaki, N., and Dixit, V. M. (2024). Cell death. *Cell*, 187 (2), 235–256. doi:10.1016/j.cell.2023.11.044
- Nian-Wu, H., Yan, Z., Ling, G., Jun, S., and Xing-Bin, Y. (2012). Antioxidant, antiproliferative, and pro-apoptotic activities of a saponin extract derived from the roots of Panax notoginseng (Burk.) F.H. Chen. *J. Med. Food* 15 (4), 350–359. doi:10.1089/jmf.2011.1801
- Okolie, C. E., Cockayne, A., Penfold, C., and James, R. (2013). Engineering of the LukS-PV and LukF-PV subunits of Staphylococcus aureus Pantone-Valentine leukocidin for diagnostic and therapeutic applications. *BMC Biotechnol.* 13, 103. doi:10.1186/1472-6750-13-103
- Oscarsson, J., Tegmark-Wisell, K., and Arvidson, S. (2006). Coordinated and differential control of aureolysin (aur) and serine protease (sspA) transcription in Staphylococcus aureus by sarA, rot and agr (RNAIII). *Int. J. Med. Microbiol. IJMM* 296 (6), 365–380. doi:10.1016/j.ijmm.2006.02.019
- Paiva, T. O., Geoghegan, J. A., and Dufrene, Y. F. (2023). High-force catch bonds between the Staphylococcus aureus surface protein SdrE and complement regulator factor H drive immune evasion. *Commun. Biol.* 6 (1), 302. doi:10.1038/s42003-023-04660-1



- Palavecino, E. L. (2020). Clinical, epidemiologic, and laboratory aspects of methicillin-resistant *Staphylococcus aureus* infections. *Methods Mol. Biol. Clift. N.J.* 2069, 1–28. doi:10.1007/978-1-4939-9849-4\_1
- Peacock, S. J., and Paterson, G. K. (2015). Mechanisms of methicillin resistance in *Staphylococcus aureus*. *Annu. Rev. Biochem.* 84, 577–601. doi:10.1146/annurev-biochem-060614-034516
- Peschel, A., and Otto, M. (2013). Phenol-soluble modulins and staphylococcal infection. *Nat. Rev. Microbiol.* 11 (10), 667–673. doi:10.1038/nrmicro3110
- Rickard, J. A., O'Donnell, J. A., Evans, J. M., Lalaoui, N., Poh, A. R., Rogers, T., et al. (2014). RIPK1 regulates RIPK3-MLKL-driven systemic inflammation and emergency hematopoiesis. *Cell* 157 (5), 1175–1188. doi:10.1016/j.cell.2014.04.019
- Rong, L., Chen, Y., He, M., and Zhou, X. (2009). Panax notoginseng saponins attenuate acute lung injury induced by intestinal ischaemia/reperfusion in rats. *Respirol. Carlt. Vic.* 14 (6), 890–898. doi:10.1111/j.1440-1843.2009.01586.x
- Rungelrath, V., and DeLeo, F. R. (2021). *Staphylococcus aureus*, antibiotic resistance, and the interaction with human neutrophils. *Antioxidants and Redox Signal.* 34 (6), 452–470. doi:10.1089/ars.2020.8127
- Rungelrath, V., Porter, A. R., Malachowa, N., Freedman, B. A., Leung, J. M., Voyich, J. M., et al. (2021). Further insight into the mechanism of human PMN lysis following phagocytosis of *Staphylococcus aureus*. *Microbiol. Spectr.* 9 (2), e0088821. doi:10.1128/Spectrum.00888-21
- Sheng-Yan, H., Wen, L., Chu-Man, H., Hui-Mei, H., Qi-Long, C., Yun-Xiao, L., et al. (2024). Enhancing antioxidant levels and mitochondrial function in porcine oocyte maturation and embryonic development through notoginsenoside R1 supplementation. *Reprod. Domest. Anim.* 59 (6), e14631. doi:10.1111/rda.14631
- Singh, A. K., Praharaj, M., Lombardo, K. A., Yoshida, T., Matoso, A., Baras, A. S., et al. (2022). Re-engineered BCG overexpressing cyclic di-AMP augments trained immunity and exhibits improved efficacy against bladder cancer. *Nat. Commun.* 13 (1), 878. doi:10.1038/s41467-022-28509-z
- Song, H.-S., Bhatia, S. K., Choi, T.-R., Gurav, R., Kim, H. J., Lee, S. M., et al. (2024). Increased antibiotic resistance of methicillin-resistant *Staphylococcus aureus* USA300  $\Delta$ psm mutants and a complementation study of  $\Delta$ psm mutants using synthetic phenol-soluble modulins. *J. Microbiol. Biotechnol.* 31 (1), 115–122. doi:10.4014/jmb.2007.07034
- Tenover, F. C., and Goering, R. V. (2009). Methicillin-resistant *Staphylococcus aureus* strain USA300: origin and epidemiology. *J. Antimicrob. Chemother.* 64 (3), 441–446. doi:10.1093/jac/dkp241
- Tewari, R., Sharma, V., Koul, N., Ghosh, A., Joseph, C., Hossain, Sk U., et al. (2009). Ebselen abrogates TNF $\alpha$  induced pro-inflammatory response in glioblastoma. *Mol. Oncol.* 3 (1), 77–83. doi:10.1016/j.molonc.2008.10.004
- Turgay, K., Hamoen, L. W., Venema, G., and Dubnau, D. (1997). Biochemical characterization of a molecular switch involving the heat shock protein ClpC, which controls the activity of ComK, the competence transcription factor of *Bacillus subtilis*. *Genes and Dev.* 11 (1), 119–128. doi:10.1101/gad.11.1.119
- Valko, M., Leibfritz, D., Moncol, J., Cronin, M. T., Mazur, M., and Telser, J. (2007). Free radicals and antioxidants in normal physiological functions and human disease. *Int. J. Biochem. Cell Biol.* 39 (1), 44–84. doi:10.1016/j.biocel.2006.07.001
- Venkatasubramaniam, A., Kanipakala, T., Ganjbaksh, N., Mehr, R., Mukherjee, I., Krishnan, S., et al. (2018). A critical role for HlgA in *Staphylococcus aureus* pathogenesis revealed by A switch in the SaeRS two-component regulatory system. *Toxins (Basel)* 10 (9), 377. doi:10.3390/toxins10090377
- Wang, H., Sun, L., Su, L., Rizo, J., Liu, L., Wang, L. F., et al. (2014). Mixed lineage kinase domain-like protein MLKL causes necrotic membrane disruption upon phosphorylation by RIP3. *Mol. Cell* 54 (1), 133–146. doi:10.1016/j.molcel.2014.03.003
- Wang, L., Huang, Y., Yin, G., Wang, J., Wang, P., Chen, Z.-Y., et al. (2020). Antimicrobial activities of Asian ginseng, American ginseng, and notoginseng. *Phytotherapy Res. PTR* 34 (6), 1226–1236. doi:10.1002/ptr.6605
- Wang, L., Yang, X., Yu, X., Yao, Y., and Ren, G. (2013). Evaluation of antibacterial and anti-inflammatory activities of less polar ginsenosides produced from polar ginsenosides by heat-transformation. *J. Agric. Food Chem.* 61 (50), 12274–12282. doi:10.1021/jf404461q
- Wang, P., Hou, Y., Zhang, W., Zhang, H., Che, X., Gao, Y., et al. (2019). Pseudoginsenoside-F11 attenuates lipopolysaccharide-induced acute lung injury by suppressing neutrophil infiltration and accelerating neutrophil clearance. *Inflammation* 42 (5), 1857–1868. doi:10.1007/s10753-019-01047-5
- Wang, R., Braughton, K. R., Kretschmer, D., Bach, T. H., Queck, S. Y., Li, M., et al. (2007). Identification of novel cytolytic peptides as key virulence determinants for community-associated MRSA. *Nat. Med.* 13 (12), 1510–1514. doi:10.1038/nm1656
- Warheit-Niemi, H. I., Edwards, S. J., SenGupta, S., Parent, C. A., Zhou, X., O'Dwyer, D. N., et al. (2022). Fibrotic lung disease inhibits immune responses to staphylococcal pneumonia via impaired neutrophil and macrophage function. *JCI Insight* 7 (4), e152690. doi:10.1172/jci.insight.152690
- Wei, R., Xu, L. W., Liu, J., Li, Y., Zhang, P., Shan, B., et al. (2017). SPATA2 regulates the activation of RIPK1 by modulating linear ubiquitination. *Genes Dev.* 31 (11), 1162–1176. doi:10.1101/gad.299776.117
- Weinlich, R., Oberst, A., Beere, H. M., and Green, D. R. (2017). Necroptosis in development, inflammation and disease. *Nat. Rev. Mol. Cell Biol.* 18 (2), 127–136. doi:10.1038/nrm.2016.149
- Wright, H. L., Moots, R. J., Bucknall, R. C., and Edwards, S. W. (2010). Neutrophil function in inflammation and inflammatory diseases. *Rheumatology* 49 (9), 1618–1631. doi:10.1093/rheumatology/keq045
- Xiong, Y., Chen, L., Man, J., Hu, Y., and Cui, X. (2019). Chemical and bioactive comparison of Panax notoginseng root and rhizome in raw and steamed forms. *J. Ginseng Res.* 43 (3), 385–393. doi:10.1016/j.jgr.2017.11.004
- Xiong, Y., Halima, M., Che, X., Zhang, Y., Schaaf, M. J. M., Li, M., et al. (2022). Steamed panax notoginseng and its saponins inhibit the migration and induce the apoptosis of neutrophils in a zebrafish tail-fin amputation model. *Front. Pharmacol.* 13, 946900. doi:10.3389/fphar.2022.946900
- Xue, T., You, Y., Shang, F., and Sun, B. (2012). Rot and Agr system modulate fibrinogen-binding ability mainly by regulating clfB expression in *Staphylococcus aureus* NCTC8325. *Med. Microbiol. Immunol.* 201 (1), 81–92. doi:10.1007/s00430-011-0208-z
- Yang, C., Qu, L., Wang, R., Wang, F., Yang, Z., and Xiao, F. (2024). Multi-layered effects of Panax notoginseng on immune system. *Pharmacol. Res.* 204, 107203. doi:10.1016/j.phrs.2024.107203
- Yang, W., Liu, J., Blažeković, B., Sun, Y., Ma, S., Ren, C., et al. (2018). *In vitro* antibacterial effects of Tanreqing injection combined with vancomycin or linezolid against methicillin-resistant *Staphylococcus aureus*. *BMC Complement. Altern. Med.* 18 (1), 169. doi:10.1186/s12906-018-2231-8
- Yoshimura, T., and Takahashi, M. (2007). IFN-gamma-mediated survival enables human neutrophils to produce MCP-1/CCL2 in response to activation by TLR ligands. *J. Immunol.* 179 (3), 1942–1949. doi:10.4049/jimmunol.179.3.1942
- Zhang, J., Sun, Y., Wang, Y., Lu, M., He, J., Liu, J., et al. (2014). Non-antibiotic agent ginsenoside 20(S)-Rh2 enhanced the antibacterial effects of ciprofloxacin *in vitro* and *in vivo* as a potential NorA inhibitor. *Eur. J. Pharmacol.* 740, 277–284. doi:10.1016/j.ejphar.2014.07.020
- Zhang, L., Wen, B., Bao, M., Cheng, Y., Mahmood, T., Yang, W., et al. (2021). Andrographolide sulfonate is a promising treatment to combat methicillin-resistant *Staphylococcus aureus* and its biofilms. *Front. Pharmacol.* 12, 720685. doi:10.3389/fphar.2021.720685
- Zhang, L., Yang, W., Chu, Y., Wen, B., Cheng, Y., Mahmood, T., et al. (2022). The inhibition effect of linezolid with reynanin mixture on MRSA and its biofilm is more significant than that of linezolid alone. *Front. Pharmacol.* 12, 766309. doi:10.3389/fphar.2021.766309
- Zhang, Z., Chen, L., Cui, X., Zhang, Y., Hu, Y., Wang, C., et al. (2019). Identification of anti-inflammatory components of raw and steamed Panax notoginseng root by analyses of spectrum-effect relationship. *RSC Adv.* 9 (31), 17950–17958. doi:10.1039/c9ra00906j
- Zhou, R., Tardivel, A., Thorens, B., Choi, I., and Tschopp, J. (2010). Thioredoxin-interacting protein links oxidative stress to inflammasome activation. *Nat. Immunol.* 11 (2), 136–140. doi:10.1038/ni.1831
- Zhou, Y., Niu, C., Ma, B., Xue, X., Li, Z., Chen, Z., et al. (2018). Inhibiting PSMa-induced neutrophil necroptosis protects mice with MRSA pneumonia by blocking the agr system. *Cell Death Dis.* 9 (3), 362. doi:10.1038/s41419-018-0398-z